American Mineralogist, Volume 83, pages 669–684, 1998

The systematics of Cr^{3+} and Cr^{2+} partitioning between olivine and liquid in the presence of spinel

Ben Hanson* and John H. Jones†

Planetary Science Branch, SN2, Lyndon B. Johnson Space Center, National Aeronautics and Space Administration, Houston, Texas 77058, U.S.A.

Abstract

The partitioning behavior of Cr into olivine in basaltic systems has been parameterized and can now be modeled over a wide range of redox conditions and liquid compositions. The Cr^{2+}/Cr^{3+} in spinel-saturated experimental systems can be estimated based on a simple model of Cr solubility in basalt. Fe^{3+} appears to suppress the presence of Cr^{2+} in basaltic systems. We predict that, in Fe-free systems, all Cr is trivalent at log $f_{O_2} = -3$ (i.e., QFM+3 to QFM+4), whereas all Cr is trivalent at approximately Ni-NiO(QFM+1) in Fe-bearing systems. Cr^{2+} predominates under redox conditions <IW-1 in both Fe-bearing and Fe-free systems.

$D_{Cr^{2+}}$ and $D_{Cr^{3+}}$ (olivine/liquid) have been determined in various liquid compositions and temperatures. $D_{Cr^{3+}}$ (i.e., $f_{O_2} \geq$ QFM, appropriate for most terrestrial or martian basalts) strongly covaries with the ratio of non-bridging oxygens to tetrahedrally coordinated cations (NBO/T) (Mysen 1983) and can be estimated using the equation

$$D_{Cr^{3+}}^{(ol/liq)} = -0.39 \cdot \frac{NBO}{T} + 1.29.$$

This relationship appears to be valid over the entire pressure range of olivine stability, from 1 atm to 15 GPa.

$D_{Cr^{2+}}$ (i.e., $\leq$ IW-1, appropriate for lunar and some asteroidal basalts) is sensitive to liquid composition and temperature and can be estimated using either

$$D_{Cr^{2+}}^{(ol/liq)} = 0.24 \cdot D_{Mg}^{(ol/liq)} - 0.07$$

or

$$D_{Cr^{2+}}^{(ol/liq)} = 0.66 \cdot \left[\frac{10{,}000}{T(K)}\right] - 4.48.$$

The $1/T$ equation is probably only valid at 1 atm pressure, but the D_{Mg} equation may be useful at higher pressures as well. The Cr content of spinel-saturated liquids is a function of temperature, composition, and f_{O_2}. However, the Cr content of spinel-saturated liquids is buffered by spinel and is insensitive to the bulk Cr content of the system (e.g., Roeder and Reynolds 1991). Therefore, the Cr content of a crystallizing, spinel-saturated basalt cannot be modeled using Raleigh fractionation models.

Introduction

The behavior of Cr in basaltic systems has been of great interest because Cr is an element that is compatible in several minerals that crystallize from basaltic magmas and it exists in multiple valence states. Cr is thought to exist primarily as Cr^{3+} under terrestrial redox conditions [i.e., near the quartz-fayalite-magnetite oxygen buffer (QFM)] and primarily as Cr^{2+} under reducing conditions such as those proposed for the crystallization of lunar magmas (Schreiber and Haskin 1976). The different partitioning behavior of Cr^{2+} and Cr^{3+} in basalts is thought to be reflected in the generally higher Cr content of lunar magmas in comparison with their terrestrial counterparts (e.g., Schreiber and Haskin 1976; Bell 1970; Taylor 1975). There are, however, some details regarding Cr behavior in basalts that remain to be addressed. In our survey of previous work (see below), we were struck by what appeared to be a lack of agreement between different experimental studies in terms of the Cr-partitioning data between olivine and liquid. Moreover, in some studies there appeared to be a lack of internal consistency. Some of these problems remain. We show below, how-

* Present address: Corning Incorporated, SP-FR-18, Corning, New York 14831, U.S.A.

† E-mail: john.h.jones1@jsc.nasa.gov

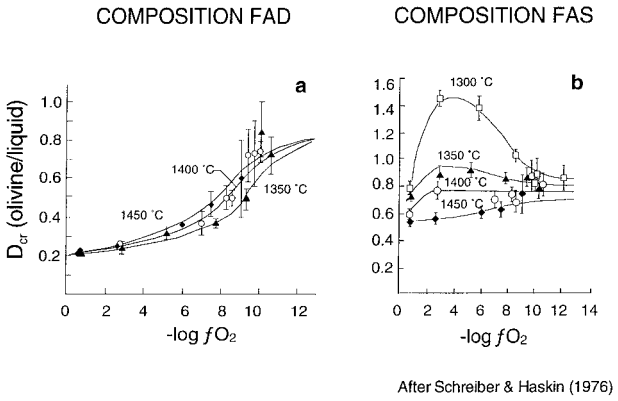

FIGURE 1. Plot of D_{Cr} (olivine/liquid) as a function of T and f_{O_2} in the Fe-free systems FAD and FAS (modified from Schreiber and Haskin 1976; Fig. 7, page 1243). D_{Cr} is the weight ratio of Cr in olivine to Cr in the glass. Note the difference in functional form between the two compositional systems.

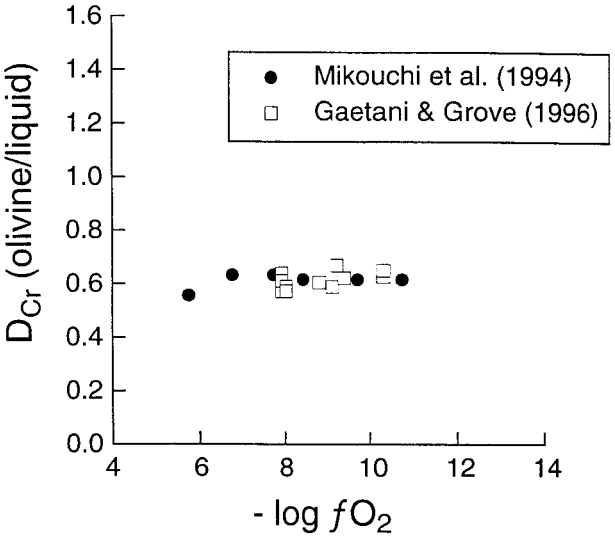

FIGURE 2. Plot of D_{Cr} (olivine/liquid) in Fe-bearing systems from two different data sets from the literature. The Gaetani and Grove (1997) experiments were performed on a komatiite bulk composition at 1350 °C and the Mikouchi et al. (1994) experiments were performed on an angrite bulk composition at 1400 °C. Note that, in contrast to the SH(1976) data shown in Figure 1, D_{Cr} does not change with oxygen fugacity, temperature, or liquid composition.

ever, that a large body of experimental work can be systematized and, thus, our concerns have been greatly alleviated. First, however, let us point out some of the apparent problems that led to this study.

For example, Figure 1 shows D_{Cr} (olivine/liquid) as a function of f_{O_2} from Schreiber and Haskin (1976). Note the large change in D_{Cr} (olivine/liquid) as a function of f_{O_2} in both of these Fe-free systems. D_{Cr} (olivine/liquid) increases with decreasing f_{O_2} in the system forsterite-anorthite-diopside (FAD), but decreases with decreasing f_{O_2} in the system forsterite-anorthite-silica (FAS). Note also that D_{Cr} (olivine/liquid) is greatly affected by temperature in one system, but not in the other. These data apparently indicate that D_{Cr} (olivine/liquid) is very sensitive to f_{O_2} temperature, and liquid composition. Although we expect D_{Cr} (olivine/liquid) to change with temperature and liquid composition, we expect the functional form of the curves to be similar in both FAS and FAD. For example, we would not expect temperature to have such a significant effect on D_{Cr} (olivine/liquid) in one compositional system, but to have virtually no effect on D in the other.

Figure 2 shows D_{Cr} (olivine/liquid) as a function of f_{O_2} in Fe-bearing systems from Gaetani and Grove (1997) and from Mikouchi et al. (1994). In contrast to the data from Schreiber and Haskin, these data show no variation in D_{Cr} (olivine/liquid) with f_{O_2}. The lack of variation in D_{Cr} (olivine/liquid) in Fe-bearing systems, coupled with the large variations observed in the Fe-free systems, suggested to us the following possibilities:

(1) Cr^{2+} does not exist under geologically relevant redox conditions, and the apparent systematic variation in D_{Cr} with f_{O_2} observed by Schreiber and Haskin (1976) was the result of experimental or analytical problems.

(2) Cr^{2+} exists in Fe-free systems, but does not exist in basaltic systems where significant quantities of Fe^{3+} are present (e.g., Schreiber and Haskin 1976).

(3) Cr exists in two valence states in the experiments on the Fe-bearing basalts shown in Figure 2, but $D_{Cr^{2+}}$ and $D_{Cr^{3+}}$ (olivine/liquid) are so similar that they cannot be distinguished.

We have performed a series of experiments in various Fe-free and Fe-bearing compositions over a wide range in f_{O_2} (>18 log units) and have determined values for distribution coefficients for Cr^{2+} and Cr^{3+} into olivine. We have also characterized the variation in D_{Cr} as a function of f_{O_2} and liquid composition. The data from the spinel-saturated experiments were used to develop a model for calculating Cr^{2+}/Cr^{3+} as a function of f_{O_2} in both Fe-free and Fe-bearing systems and for evaluating the effect of Fe^{3+} on the Cr-redox behavior in natural basalts. The model allows the prediction of the values of $D_{Cr^{3+}}$ (olivine/liquid) as a function of liquid composition (in Fe-free and Fe-bearing systems) to within 10% relative, regardless of temperature, and of $D_{Cr^{2+}}$ as a function of temperature.

From this point forward we refer to Schreiber and Haskin (1976) as SH(1976). This paper stems from the Ph.D. thesis of Schreiber (1976), from which we obtained the data and many experimental details that were omitted from Schreiber and Haskin (1976). Because mostly olivine partitioning results are presented, D_{Cr} refers to the partition coefficient of Cr between olivine and melt unless otherwise noted.

EXPERIMENTAL AND ANALYTICAL DETAILS

Starting compositions

The compositions of the starting materials used in this study are listed in Table 1. These compositions were syn-

TABLE 1. Compositions of the experimental systems

	FAD1a	FAD1b	FAD2	FAD3	FAS1	MORB1	MORB2	MORB3a	MORB3b	YBG*	BG†	PPG‡
SiO_2	46.09	46.09	49.96	49.63	54.20	48.81	51.54	49.62	49.62	42.9	34.0	49.0
TiO_2	0	0	0	0	0	0.83	2.16	3.71	3.71	3.48	16.4	0.63
Al_2O_3	12.03	12.03	11.74	10.96	14.63	17.51	13.26	11.06	11.06	8.30	4.6	14.0
MgO	27.91	27.91	17.62	19.04	22.74	9.51	6.14	4.27	4.27	13.5	13.3	10.7
MnO	0	0	0	0	0	0	0.22	0.27	0.27	0.27	0.31	0.2
FeO§	0	0	0	0	0	7.45	13.48	18.85	18.85	22.1	24.5	14.0
CaO	13.58	13.58	20.68	19.93	8.00	12.88	10.79	9.24	9.24	8.50	6.9	11.2
Na_2O	0	0	0	0	0	2.13	2.32	2.49	2.49	0.45	0.23	0
K_2O	0	0	0	0	0	0.02	0.11	0.19	0.19	0	0.16	0
$Cr_{(ppm)}$	1500	3000	3500	3500	3500	3000	3000	1500	3000	4037	6295	2740
$V_{(ppm)}$	0	0	0	0	0	3000	3000	3000	3000	3000	3000	5000

Note: FAD3 and FAS1 were synthesized in an attempt to reproduce the results of Schreiber and Haskin (1976).
* Apollo 15 yellow brown glass (Delano 1986).
† Apollo 14 black glass (Delano 1986).
‡ "Pristine picritic glass" of Jones and Delano (1989).
§ Total iron reported as FeO.

thesized using reagent-grade oxide powders that were mixed by grinding in ethanol for a minimum of 1 h in an agate mortar and pestle.

We have investigated Cr-partitioning in both Fe-free and Fe-bearing systems. The bulk compositions chosen for the Fe-free experiments (Fig. 3) fall within FAD and FAS haplobasaltic systems. The compositions FAD3 and FAS1 were chosen to reproduce the results of SH(1976). Because we were particularly interested in verifying their D_{Cr} results at lower temperatures (1300–1350 °C), we chose a starting composition with a liquidus temperature closer to the temperature of interest. Our compositions are only 30–60 °C below the liquidus at 1320 °C [as opposed to 150–200 °C in the experiments of SH(1976)]. Thus, our experiments contain fewer crystals, but have glass compositions similar to those of SH(1976). Although the lowest-temperature FAD experiment from SH(1976) is 1350 °C, we chose to perform our experiment at 1320 °C to directly compare the results to our other experiments. The weak temperature dependence of D_{Cr} in FAD (Fig. 1) suggested that this small difference in temperature would have a negligible effect. As shown below, this turned out not to be true.

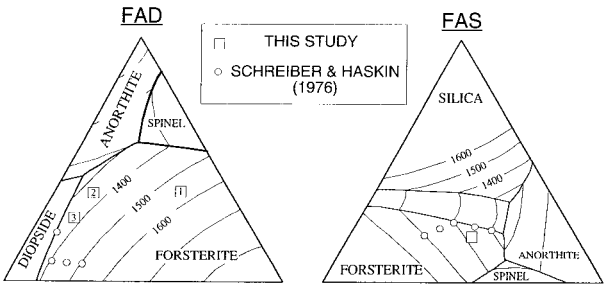

FIGURE 3. Ternary diagrams showing the locations of the bulk compositions used in this study. The numbers in the symbols in FAD correspond to FAD1, FAD2, and FAD3, from Table 1. The liquid compositions of the experiments from SH(1976) are shown for comparison. The highest temperature Schreiber and Haskin points represent their two bulk compositions [i.e., the SH(1976) FAS 1350 °C liquid was produced experimentally from a starting composition that had a liquidus of ~1500 °C].

We also combine data from several Fe-bearing systems from this study and from the literature. The bulk compositions of our Fe-bearing systems are also listed in Table 1. The literature data comes from Mikouchi et al. (1994), Longhi and Pan (1989), Herzberg and Zhang (1996), Gaetani and Grove (1997), Delano (unpublished data), Heubner et al. (1976), Akella et al. (1976), Jurewicz et al. (1993a), and Walker et al. (1977). The electron microprobe data of Longhi and Pan (1989) were obtained with relatively low beam currents (20 nA at 15 keV) and short counting times (20 s), therefore, the uncertainties in their Cr_2O_3 numbers are relatively large (10–20% relative). We have reanalyzed the experimental products of Longhi and Pan to obtain higher precision data for Cr. Our results agree with those of Longhi and Pan (1989) within their stated uncertainties.

Pt-loop gas-mixing experiments at 1 bar

Experiments were performed both at the Johnson Space Center (JSC) and at the State University of New York at Albany (SUNY). Experiments were performed by holding the powdered starting material in the hot spots of Deltech gas-mixing furnaces controlled to within ±2 °C of the desired temperatures. In the SUNY experiments, Fe loss to Pt loops in Fe-bearing experiments was minimized by preparing Pt-Fe alloy loops with a composition calculated using the method described by Grove (1981). Pre-weighed, pre-formed platinum wire (0.005 inch diameter) loops were electroplated with Fe^0 in a ferrous sulfide bath until the appropriate Fe/Pt ratio was achieved. The loops were then annealed at 1300 °C for at least 24 h at 1 log unit below the iron-wüstite oxygen buffer (IW-1), which resulted in homogeneous Pt-Fe alloys. At JSC, loops were saturated with Fe and Cr by performing multiple saturation experiments (e.g., Fig. 4).

Temperatures were monitored by thermocouples (calibrated against the melting temperature of Au) that were placed adjacent to the samples. The redox conditions

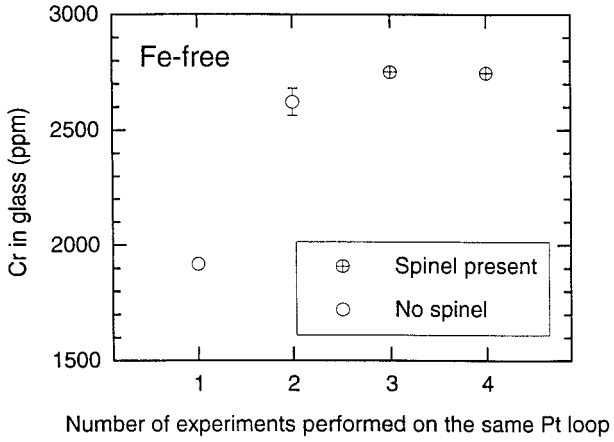

FIGURE 4. Plot of the results of four replicate experiments performed on the same Pt loop using composition FAD1. Four identical experiments were performed and residual material was cleaned from the loops between experiments by soaking in HF. After two experiments the Pt loop is saturated with Cr.

within the furnaces during the experiments run at intermediate f_{O_2} (i.e., 10^{-3} to IW-1) were controlled by mixing CO and CO_2 in appropriate proportions. At SUNY, the redox conditions were monitored using a ZrO_2 oxygen sensor placed in the furnace adjacent to the sample. Oxygen sensors were calibrated using iron-wüstite (IW) and nickel-nickel oxide (NNO) solid buffers placed within the O sensors. At JSC, the redox conditions in the furnaces were measured using a ZrO_2 oxygen sensor placed in a remote furnace (Jurewicz et al. 1993b) and the system was calibrated using a 50/50 mixture of CO and CO_2. The O sensor is placed in a remote furnace, and gases are routed selectively from the sample furnaces into the remote furnace when the redox conditions are to be measured. Thus, only one sensor is needed to measure the oxygen fugacity in all of the furnaces in the lab. The measured f_{O_2} in both labs is thought to be accurate to within 0.1 (1σ) log units (Jurewicz et al. 1993b). After the experiments, the samples were quenched in water.

Schreiber (1976) reported Cr loss and ''mobility'' in his experiments. Cr loss was slowest at intermediate redox conditions near QFM, with greater losses occurring at both low (IW) and high (air) values of f_{O_2}. We have also observed Cr volatility in our Fe-free experiments, but only for those run in air. An initial Pt-loop experiment was performed in air at 1320 °C on the Fe-free composition FAD1b (Table 1). After quench, no spinel was present in the sample, even though spinel was present in all other experiments in the FAD1 system from air to f_{O_2} = IW-1. Because olivine (with a value of $D_{Cr} \leq 1$) was the only mineral present and spinel (picrochromite; the primary reservoir for Cr in these experiments) was absent, the Cr concentration in the liquid should have been greater than the amount in the bulk composition (e.g., 6000

TABLE 2. Phase compositions from selected experiments (top portion of table); also listed are the values of D_{Cr} (olivine/liquid) and Cr_2O_3-content of glasses [i.e., Cr(l)] as a function of f_{O_2} from all experiments (bottom portion of table)

	FAD1b 1320 °C*			FAD2 1320 °C			FAD3 1320 °C		
	Glass	Olivine	Spinel	Glass	Olivine	Spinel	Glass	Olivine	Spinel
SiO_2	48.38(9)	42.9(2)	0.4(2)	50.4(4)	42.9(4)	0.29(7)	50.3(3)	42.6(2)	0.38(8)
Al_2O_3	16.75(9)	0.09(2)	33.6(4)	12.42(7)	0.06(1)	19.9(2)	11.4(3)	0.05(1)	15(1)
MgO	14.9(2)	56.1(3)	24.1(2)	15.36(5)	55.8(2)	23.2(3)	16.2(2)	55.8(3)	21.0(8)
CaO	18.75(8)	0.15(4)	0.43(1)	21.81(6)	0.79(2)	0.61(7)	21.7(3)	0.79(2)	0.57(6)
Cr_2O_3	0.125(4)	0.080(2)	41.7(6)	0.22(1)	0.12(1)	56.6(3)	0.227(9)	0.10(1)	62(2)
Total	98.9	100.1	100.2	100.2	99.7	100.6	99.8	99.3	99.0
Phases†	fsl	—	—	fsl	—	—	fds	—	—
NBO/T‡	1.0	—	—	1.22	—	—	1.27	—	—
	log f_{O_2}	D_{Cr} f/l	Cr (l)	log f_{O_2}	D_{Cr} f/l	Cr (l)	log f_{O_2}	D_{Cr} f/l	Cr (l)
	−0.68	0.5(1)	0.177(5)	−3	0.54(7)	0.22(1)	−3.0	0.45(6)	0.227(9)
	−3.0	0.64(3)	0.125(4)	—	—	—	−7.2	0.50(4)	0.257(7)
	−5.9	0.68(5)	0.140(7)	—	—	—	−9.0	0.59(3)	0.342(8)
	−7.64	0.69(4)	0.174(3)	—	—	—	−10.5	0.63(1)	0.47(1)
	−7.20 R	0.67(6)	0.148(7)	—	—	—	−10.5 R	0.62(4)	0.633(7)
	−7.92	0.69(3)	0.177(4)	—	—	—	−15.3(3)§	0.73(1)	0.60(2)
	−8.64	0.70(2)	0.223(2)	—	—	—	—	—	—
	−10.51	0.71(1)	0.394(7)	—	—	—	—	—	—
	−14.3(3)§	0.73(1)	0.292(5)						
	≤−18	0.76(9)	0.060(7)	—	—	—	—	—	—

Note: Major element compositions of phases within experiments run at $f_{O_2} = 10^{-3}$ are shown for all compositions. Numbers in parenthesis are the 1σ standard deviation and are equal to the last decimal place. R represents reversal experiments.

* Note that the compositions of the identical experiments on composition FAD1a and FAD1b are nearly identical so the data for FAD1a were not presented here.

† Silicate phases present in all charges regardless of f_{O_2} except spinel. Spinel was not present in experiments run at $f_{O_2} = 10^{-18}$. l = liquid, s = spinel, f = forsterite, e = enstatite, and d = diopside.

‡ Ratio of non-bridging oxygen atoms to tetrahedrally coordinated cations after Mysen (1984).

§ The experiments performed on Fe^0 loops contained FeO dissolved in the silicates. The liquids from these experiments contained 1.86 (±0.05), 0.6 (±0.02), and 2.50 (±0.08) wt% FeO for the composition FAD1b, FAD3, and FAS, respectively. The uncertainty on the f_{O_2} calculations, which were calculated based on the FeO-contents of the liquids, are estimated from the data of Hillgren (1993).

ppm, Table 1) if the system was chemically closed. The actual Cr content measured in the glass was 130 ± 40 ppm. In addition to the low Cr content of the liquid, the olivine was zoned with respect to Cr, with the cores being enriched relative to the rims. The low Cr content of the liquid, the absence of spinel, the absence of Cr in the Pt loop, and the zoning profile in olivine all suggest that Cr was lost from the experiment through volatilization. Because Cr volatility was only observed in the experiments performed in air and because the partition coefficients are consistent with the presence of Cr^{6+} (see below), we conclude that Cr^{6+} was the volatile Cr species in these experiments. To minimize volatilization in experiments that were run in air, samples were placed in $Pt_{95}Au_5$ tubes with a pinhole leak. This technique successfully minimized the volatilization of Cr as indicated by the presence of spinel and by the absence of measurable zoning in olivine.

Schreiber (1976) ruled out Cr loss to Pt at low f_{O_2} because he measured no appreciable Cr in the platinum tubes after his experiments. However, we found that appreciable Cr is lost to Pt from Fe-free systems during 1 atm experiments performed under reducing conditions. The Pt can be saturated with Cr by running several successive, identical experiments on the same loop. We performed a series of experiments at 1320 °C and IW on the same loop using composition FAD1b (Table 1) to determine how many successive experiments were needed to saturate Pt loops. Figure 4 shows the Cr content of the resulting glasses. The Cr content of the glass systematically increased to a maximum abundance after the second experiment on this loop. Spinel, the major sink for Cr in these experiments, was not present in the sample until after the second experiment, at which point the loop became saturated with Cr. Based on these results, at least two successive experiments were performed on the same loop, before a third experiment performed on that loop was considered acceptable for analysis. Approximately 3 wt% Cr was measured in a Pt loop after the fourth consecutive experiment, resulting in a partition coefficient for Pt/silicate liquid in this experiment of approximately 100. Qualitative analyses of loops indicated that no appreciable Cr was lost to the Pt in the Fe-bearing experiments. The loss of Fe to the loop is favored over Cr and apparently inhibits Cr reduction.

Reversal experiments were performed to determine the extent to which our experimental results represent chemical equilibrium between the silicate liquid and the solid phases. The reversal experiments on Pt loops were initially held for 2 d at an f_{O_2} of 10^{-3} or IW, after which the f_{O_2} was changed to either IW or 10^{-3} and held for 6 d before quenching. Typically, the compositions of the silicate phases in the reversal experiments were identical, within analytical uncertainty, to those in the single-condition experiments (Table 2). The reversal experiments not only demonstrate the close approach to equilibrium between minerals and liquid, but also between the liquid and the Pt loop. The long duration of these experiments also demonstrates that minimal Cr was lost by volatility during our Pt-loop experiments at $f_{O_2} < 10^{-3}$.

One of the goals of these experiments was to determine the difference in olivine/silicate melt partition coefficients for different Cr redox states. If chromium occurs as both Cr^{2+} and Cr^{3+} in the same experimental sample, the measured D_{Cr} is the sum of $D_{Cr^{2+}}$ and $D_{Cr^{3+}}$, making the individual determination of $D_{Cr^{2+}}$ and $D_{Cr^{3+}}$ impossible if the concentrations of both Cr species are not known. To overcome this difficulty, the redox conditions must be either reducing or oxidizing so that most of the element exists in one redox state. For the oxidized species, experiments were run in air ($\log f_{O_2} = -0.68$) or pure CO_2 ($\log f_{O_2} = -3.0$) at 1300–1320 °C as described above. Extremely reducing conditions were used in an attempt to ensure the predominance of the most-reduced species. These reducing experiments were performed on Fe-free compositions using two different experimental procedures: (1) gas-mixing experiments run on Fe loops and (2) sealed silica-tube experiments containing graphite.

TABLE 2—*Continued.*

FAS1 1320 °C			FAS1 1300 °C		
Glass	Olivine	Spinel	Glass	Olivine	Spinel
55.3(2)	42.7(2)	0.26(3)	54.4(3)	42.7(2)	0.27(4)
17.56(7)	0.09(2)	30.2(6)	18.4(1)	0.092(6)	35.5(9)
17.1(1)	56.7(3)	23.7(2)	15.8(4)	56.3(2)	24.7(3)
10.29(5)	0.195(8)	0.27(6)	10.92(9)	0.193(7)	0.22(5)
0.137(6)	0.119(5)	44.7(6)	0.110(7)	0.096(7)	39.7(7)
100.4	99.8	99.1	99.8	99.4	100.4
fesl	—	—	fesl	—	—
0.70	—	—	0.64	—	—
log f_{O_2}	D_{Cr} f/l	Cr (l)	log f_{O_2}	D_{Cr} f/l	Cr (l)
−3	0.87(5)	0.137(6)	−3	0.87(8)	0.110(7)
−7.2	0.79(6)	0.201(8)	—	—	—
−7.2 R	0.81(5)	0.199(6)	—	—	—
−9.0	0.77(3)	0.320(5)	—	—	—
−10.5	0.73(2)	0.551(7)	—	—	—
−14.0(3)§	0.701(7)	0.509(3)	—	—	—
≤−18.0	0.71(7)	0.066(6)			—
—	—	—	—	—	—
			—	—	
—	—	—	—	—	—

Fe-loop gas-mixing experiments at 1 bar

Experiments were performed at JSC under low-f_{O_2} conditions (i.e., IW-3 to IW-5) using CO_2/CO gas mixtures in 1 atm furnaces. The experimental samples were hung on loops that were made from iron metal wire instead of platinum. Fe was used because, under these conditions, Si alloys with Pt, producing a Pt-Si liquid. Also, at these reducing conditions, C from the furnace

TABLE 3. Compositions of glass and olivine from the 1 atm experiments from this study

	PPG-1	PPG-2	YG-54	BG-54	YG-56	YBG-58	Morb1
T (°C)	1185	1200	1160	1160	1225	1230	1175
f_{O_2}	QFM	QFM	QFM	QFM	QFM	QFM	QFM
Glass							
SiO_2	48.8(3)	49.3(2)	45.6(3)	40.2(2)	44.3(3)	44.2(2)	52.8(1)
TiO_2	0.67(2)	0.65(2)	4.80(2)	11.80(4)	3.89(4)	3.83(1)	1.15(2)
Al_2O_3	14.69(7)	14.38(6)	10.70(9)	7.57(5)	9.43(9)	9.30(6)	14.3(2)
MgO	8.82(3)	9.03(4)	7.24(2)	7.68(6)	9.46(4)	9.89(3)	8.34(5)
MnO	na	na	0.27(5)	0.62(5)	0.31(4)	0.31(5)	0
FeO	14.22(7)	13.9(1)	19.7(1)	24.7(1)	21.85(7)	21.5(2)	9.45(5)
CaO	12.34(3)	12.02(4)	10.74(2)	6.57(9)	9.3(1)	9.43(4)	12.4(1)
Na_2O	na	na	0.36(1)	0.29(1)	0.31(1)	0.32(1)	1.05(7)
Cr_2O_3	0.046(2)	0.053(2)	0.078(2)	0.070(4)	0.135(5)	0.129(6)	0.087(5)
Sc_2O_3	0.543(2)	0.552(4)	0	0	0	0	0
V_2O_3	0.218(2)	0.225(4)	0.375(4)	0	0.417(4)	0.422(3)	0.164(3)
Total	100.35	100.11	99.86	99.50	99.40	99.33	99.74
Olivine							
SiO_2	39.1(4)	39.2(2)	37.6(1)	37.34(5)	38.1(2)	38.3(1)	40.1(7)
TiO_2	0.010(9)	0.006(4)	0.06(2)	0.36(9)	0.07(7)	0.05(2)	0.016(6)
Al_2O_3	0.08(1)	0.08(2)	0.050(4)	0.038(7)	0.05(1)	0.055(4)	0.06(1)
MgO	40.3(3)	40.8(2)	34.0(1)	33.4(1)	36.7(2)	37.4(1)	44.4(4)
MnO	na	na	na	na	na	na	0
FeO	20.4(2)	19.7(2)	27.1(1)	27.8(2)	23.9(3)	23.2(2)	15.0(2)
CaO	0.26(1)	0.27(2)	0.21(5)	0.05(1)	0.08(1)	0.29(3)	0.36(2)
Cr_2O_3	0.049(3)	0.050(3)	0.047(5)	0.031(6)	0.076(5)	0.076(5)	0.085(6)
Sc_2O_3	0.099(1)	0.099(2)	0	0	0	0	0
V_2O_3	0.017(4)	0.016(2)	0.026(3)	0	0.029(6)	0.022(4)	0.014(3)
Total	100.23	100.22	99.10	99.05	99.00	99.39	100.03
KD	0.31	0.31	0.29	0.26	0.28	0.29	0.30
NBO/T	0.93	0.92	1.35	2.11	1.56	1.58	0.80
DCr	1.05(7)	0.95(8)	0.60(6)	0.44(9)	0.56(4)	0.59(5)	0.98(8)

Note: All iron reported as FeO. Numbers in parenthesis are the 1σ uncertainties and are equal to the last decimal place of the measured value. ''na'' means the oxide was not measured.

atmosphere contaminates the thermocouple, which results in erroneously high-temperature measurements. Therefore, the temperature of the furnaces was adjusted before the experiments with the normal experimental apparatus equipped with a thermocouple, then the thermocouple was removed and the experiments were performed as usual. Precipitation of graphite between the sample furnace and the remote ZrO_2 oxygen sensor was found to cause significant errors in the f_{O_2} measurement for these experiments. Therefore, oxygen fugacities in these experiments were calculated using the FeO content of the silicate liquid in equilibrium with Fe metal, assuming that the activity of FeO is equal to its cation fraction in the melt and using wüstite thermodynamic data from Robie et al. (1978). Hillgren (1993) found that the f_{O_2} calculated in this way was within 0.3 log units of the measured f_{O_2} in experiments run near IW (hence the uncertainties shown in Table 2).

Sealed silica tube experiments

To achieve even more reducing conditions, an aliquot of the Cr-doped sample held in a graphite crucible was sealed in an evacuated silica tube along with a separate alumina crucible filled with chromium metal powder. Samples were hung in the hot spot of a Deltech furnace at 1310–1320 °C for 48 h and then quenched by rapidly removing the tube from the furnace and quickly placing it in water. The experimental samples were found to contain chromium metal, which had precipitated from the silicate liquid. Olivine crystals in these samples were zoned, with Cr increasing toward the rim. With hindsight, we realized that, in the evacuated tubes, C-CO (not Cr-Cr_2O_3) must have been the dominant oxygen buffer. The actual f_{O_2} was several log units below Cr-Cr_2O_3. The exact f_{O_2} is not known but, because chromium metal was present in the samples at the end of the experiments and the Cr_2O_3 abundance in the liquid was approximately 400 ppm, we can assume that the f_{O_2} within the tubes was at least three log units below the Cr-Cr_2O_3 buffer, which is approximately 10^{-15} at 1320 °C (Jurewicz et al. 1995). The C-CO buffer is very sensitive to pressure, thus during the experiments, the silica tubes slowly collapsed. This change in pressure increased the f_{O_2} within the silica tubes, which caused the chromium metal to oxidize, thereby increasing the Cr content of the silicate. Although the f_{O_2} constraints are poor for the sealed-tube experiment, this result is included here to give a rough estimate of D_{Cr} in experiments containing chromium metal.

Analytical methods

The experimental samples were analyzed using a Cameca SX-100 electron microprobe equipped with five wavelength dispersive spectrometers operated at an accelerating voltage of 15 keV. Major elements were analyzed using a cup current of 45 nA and counting times of 45 s. Minor elements were analyzed with a cup current

TABLE 3—*Continued.*

YG-51a 1175 QFM	YG-51b 1175 QFM	BG-49 1175 QFM	PPG-3 1225 IW-1	PPG-4 1200 IW-1	PPG-5d 1185 IW-1	PPG-7a 1210 IW-1
45.1(2)	45.3(2)	40.0(2)	48.78(6)	48.9(3)	50.1(2)	49.5(1)
4.09(3)	4.12(3)	11.47(4)	0.646(8)	0.65(1)	0.68(2)	0.65(1)
10.23(7)	10.35(4)	7.69(4)	13.27(5)	14.75(7)	15.1(1)	14.4(1)
7.64(5)	7.55(6)	7.87(2)	9.64(3)	9.04(1)	8.17(5)	8.84(4)
0.41(8)	0.46(5)	0.4(6)	0.20(2)	0.19(2)	0.2(1)	0.20(1)
20.4(1)	20.4(1)	24.7(1)	13.8(2)	13.64(9)	13.4(2)	13.7(1)
10.62(4)	10.81(4)	6.76(4)	11.65(3)	11.98(4)	12.44(9)	12.02(3)
0.34(3)	0.34(1)	0.30(1)	<0.02	0.02(1)	0.21(7)	0.015(5)
0.080(4)	0.079(6)	0.077(3)	0.23(1)	0.247(9)	0.32(2)	0.26(2)
0	0	0	1.369(6)	0.550(5)	0	0.551(6)
0.373(5)	0.374(1)	0	0.540(9)	0.219(5)	0	0.227(5)
99.28	99.78	99.27	100.28	100.21	100.44	100.35
37.5(2)	37.8(2)	37.1(1)	37.5(4)	38.1(2)	38.2(2)	38.2(2)
0.10(2)	0.04(1)	0.31(8)	<0.02	<0.02	<0.02	<0.02
0.049(4)	0.05(1)	0.036(3)	0.12(1)	0.09(2)	0.08(6)	0.07(1)
34.4(2)	33.9(1)	33.7(1)	40.0(2)	38.5(2)	39.1(6)	39.2(1)
na	na	na	0.20(2)	0.22(2)	0.23(1)	0.21(2)
26.7(1)	27.2(1)	27.7(1)	20.2(2)	21.9(2)	20.87(3)	20.8(1)
0.37(2)	0.306(4)	0.168(6)	0.28(1)	0.29(4)	0.28(4)	0.26(2)
0.060(7)	0.047(4)	0.042(5)	0.189(9)	0.23(1)	0.33(2)	0.25(1)
0	0	0	0.338(6)	0.109(7)	0	0.100(5)
0.032(3)	0.022(2)	0	0.346(6)	0.148(9)	0	0.136(7)
99.21	99.37	99.06	99.25	99.61	99.1	99.16
0.29	0.30	0.26	0.35	0.37	0.33	0.35
1.41	1.4	2.14	—	—	—	—
0.75(9)	0.59(6)	0.54(7)	0.83(6)	0.94(8)	1.04(6)	0.9(1)

of 100–200 nA and counting times of 120 s. Data was reduced on-line using the PAP matrix correction routine (Pouchou and Pichoir 1991). These analytical conditions provided minimum detection limits that are well below the concentrations of all elements in the samples. Each phase was analyzed at least ten times and all error bars represent the 1σ standard deviation of these ten analyses. In most cases the 1σ standard deviation agreed with the uncertainty based on counting statistics to within a factor of 2. A line scan was performed across at least one olivine from each experiment to look for inhomogeneity and to evaluate edge effects and secondary fluorescence. Line scans across olivine crystals in Fe-bearing systems showed no evidence of secondary fluorescence of Cr in the nearby glass.

Cr loss to Pt (or by volatility) or Cr gain from dissolution of chromium metal in the sealed silica-tube experiments (see below), resulted in olivine grains that were zoned with respect to Cr. Cr loss and Cr gain have been assessed by performing analytical traverses. In cases where unavoidable loss or gain of elements occurred, the Cr contents of olivine crystals were estimated by analyzing as close to their edges as possible, but far enough away so that no edge effects or fluorescence were observed. Edge effects were evaluated by observing Al abundances in olivine grains because Al is abundant in the glass but not in the olivine. An appreciable increase in Al was observed in olivine at distances <5 μm from the crystal-glass interface. Therefore, only analyses ≥ 5 μm from the edges were accepted. The Cr concentrations in some of the olivine analyses were anomalously high. These anomalous values were typically associated with high values for Al_2O_3 as well and were probably the result of included spinels that were below the polished surface of the olivine but within the excitation volume of the electron beam. Based on this interpretation, analyses that exhibited anomalously high Cr and Al abundances were discarded. Analyses of crystal-liquid pairs (separated by ~30 μm) were performed at various locations within each sample. There was no evidence for heterogeneity of the liquid or olivine compositions anywhere in the samples. Heterogeneity was only observed in olivine grains from experiments that had experienced Cr loss or gain.

The results of the analyses of the experiments on Fe-free compositions are presented in Table 2 along with the analytical uncertainties. The results of the experiments performed at QFM and ≤IW-1 on the Fe-bearing compositions are listed in Table 3. The major element data from those experiments containing only spinel and glass are not presented. The Cr content of these glasses, along with the experimental conditions, are presented in Table 4.

RESULTS

Cr systematics in spinel-saturated liquids

Figure 5 shows the Cr concentration of glass as a function of f_{O_2} for the compositions FAD1a and FAD1b, which differ only in their Cr content. The original starting material was split into two aliquots, one of which was doped with 1500 ppm Cr, and the other with 3000 ppm

TABLE 4. Oxygen fugacity and Cr content of the spinel-saturated, Fe-bearing systems MORB1, MORB2, MORB3a, and 3b (see Table 1)

MORB1 (1250 °C)		MORB2 (1200 °C)		MORB3a (1200 °C)		MORB3b (1200 °C)	
log f_{O_2}	Cr (ppm)	f_{O_2}	Cr	f_{O_2}	Cr	f_{O_2}	Cr
−3.0	452(27)	−2.7	213(46)	−2.7	106(29)	−2.7	88(13)
−7.0	626(38)	−8	606(42)	−8	581(62)	−8	478(51)
−8.0	679(41)	−10	1039(43)	−8*	465(40)	−8*	519(42)
−7.8*	731(28)	−11	1331(39)	−10	847(65)	−10	819(76)
−9.0	1180(40)	−12.0	1783(41)	−11	1154(43)	−11	1110(22)
−11.0	1534(27)			−12	1598(58)	−12	1689(66)
−11.4	1765(37)						

Note: Because the spinel is the only phase present in all experiments, the liquid compositions of each system change little with f_{O_2} with the exception of Cr. Numbers in parenthesis are the 1σ uncertainties and are equal to the last decimal place of the measured value.

* Reversal experiments initiated at IW then changed to indicated f_{O_2} after 12 to 24 h.

Cr. Pressed pellets of both the low-Cr and the high-Cr FAD mixtures were hung in the furnace at the same time to examine the effect of total Cr on the Cr content of the liquid and D_{Cr}. All of the samples contained olivine, spinel, and glass.

There are three important observations regarding these data that are relevant to this discussion. First, the Cr content of the glasses decreases systematically from IW (log $f_{O_2} = -10.5$) to log $f_{O_2} \approx -3.0$, then begins to rise again at log $f_{O_2} > -3.0$. Second, the Cr content of these spinel-saturated liquids is only slightly affected by the total Cr in the system at any given temperature or f_{O_2}. We attribute these small differences to slight changes in liquid composition resulting from the different modal abundances of spinel. Third, the composition of the spinel is constant regardless of f_{O_2} or total Cr content. The only major compositional change is the Cr content of the liquid and the olivine.

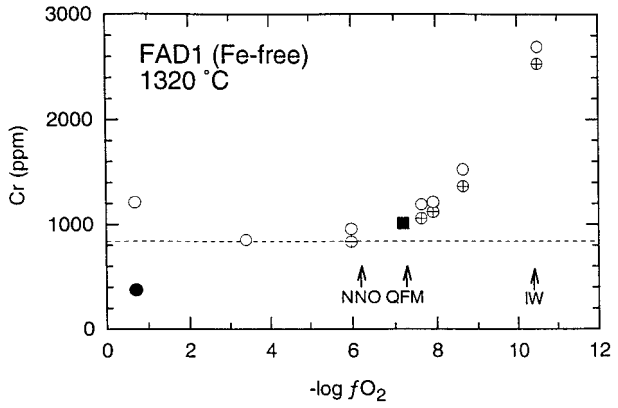

FIGURE 5. Plot of the Cr content of the glasses as a function of f_{O_2} from a series of gas-mixing experiments performed on composition FAD1 (open circles = 3000 ppm total Cr) and FAD2 (circles with crosses = 1500 ppm total Cr) at 1320 °C. The filled circle represents the experiment performed on a Pt loop in air that lost Cr due to Cr^{6+} volatility and which contained no spinel. All other samples contained spinel. The symbol directly above it represents an identical experiment run in a $Pt_{95}Au_5$ capsule exposed to air by a pinhole. No evidence for Cr loss was found in this sample. The square represents a reversal experiment on composition FAD1 changed from IW to QFM after 24 h. The dashed line at the minimum Cr abundance represents the Cr^{3+} solubility limit for this composition at this temperature. The Cr abundance above this line is a measure of Cr^{2+} or Cr^{6+} in the liquid.

The systematic behavior of Cr in spinel-saturated liquids has been described by Schreiber and Andrews (1980), Barnes (1986), Murck and Campbell (1986), and Roeder and Reynolds (1991) and can be best understood by considering Cr^{2+} and Cr^{3+} separately. For our Fe-free experiments, the cation fraction of Cr+Al of the spinel is always twice that of Mg. Therefore, the spinels contain primarily Cr^{3+}, which is an essential structural constituent of spinel. If there is not sufficient Cr^{3+} in the liquid, there will be no spinel. Conversely, if there is too much Cr^{3+}, spinel will crystallize until the Cr^{3+} saturation abundance is reached. Because the composition of the spinels remains constant, regardless of f_{O_2}, and the major-element composition of the liquid is constant, the Cr^{3+} activity of the liquid, hence the Cr^{3+} concentration (i.e., the saturation abundance), must remain constant as long as spinel is present. The increase in the Cr content of the liquid as the system is reduced from log $f_{O_2} = -3$ to IW, simply reflects the increase of Cr^{2+} in the liquid. The Cr^{2+}/Cr^{3+} in the liquid is controlled only by the externally imposed f_{O_2}. Consequently, the total Cr content of the liquid is independent of the total Cr in the system.

We assume that the increase in the Cr content of the liquid as the system is oxidized from 10^{-3} to $10^{-0.68}$ is a result of the presence of Cr^{6+}. Supporting this interpretation, as discussed below, is the rapid decrease in the olivine/liquid partition coefficient over this same interval, reflecting the highly incompatible nature of Cr^{6+} in both olivine and spinel. Cr^{6+} was measured directly by chemical titration in the Fe-free experiments of SH(1976) within this same f_{O_2} interval.

Using the simple model for Cr behavior outlined above, Cr^{2+}/Cr^{3+} can be calculated as a function of f_{O_2} in our Fe-free system. We propose that the Cr^{3+} concentration in spinel-saturated liquids is buffered at a constant level, and this level is independent of f_{O_2}. We observe that the total Cr concentration changes with changing

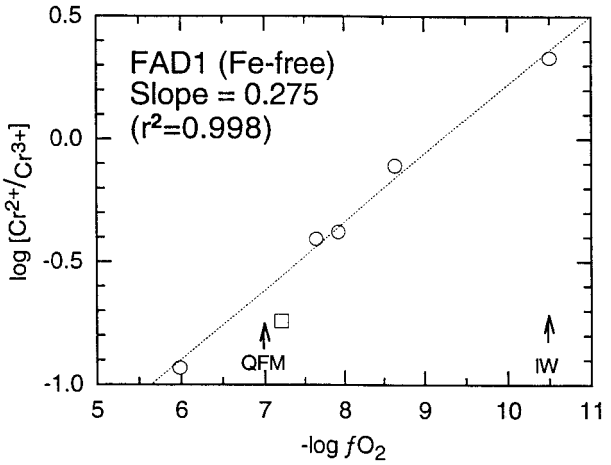

FIGURE 6. Plot of log $[Cr^{2+}/Cr^{3+}]$ vs. $-\log f_{O_2}$ for the FAD1 experiments shown in Figure 5. Cr^{2+}/Cr^{3+} was calculated using Equation 1 assuming that all Cr in excess of the Cr^{3+} solubility limit (i.e., the dashed line in Figure 5) is Cr^{2+}. Note that these data form a straight line with a slope very near to 0.25, the slope theoretically predicted for redox reactions involving one electron. The square is the reversal experiment and was not used in the regression calculation (see text).

f_{O_2}, ostensibly because of valence state changes—from Cr^{2+} under reducing conditions to Cr^{3+} at oxidizing conditions to Cr^{6+} at highly oxidizing conditions (i.e., air). Therefore, our best estimate for the spinel-buffered Cr^{3+} content of the glass in experiments at all redox conditions where spinel is present is the minimum Cr abundance in Figure 5. If we assume that the minimum Cr abundance in Figure 5 represents the spinel-saturated Cr^{3+} content, then Cr^{2+}/Cr^{3+} can be calculated for each experiment by mass balance

$$\frac{Cr^{2+}}{Cr^{3+}} = \frac{(Cr_{melt} - Cr_{min})}{Cr_{min}} \quad (1)$$

where Cr_{melt} is the measured Cr content of the liquid (i.e., $Cr^{2+} + Cr^{3+}$) and Cr_{min} is the minimum Cr content in the liquid (i.e., the abundance of Cr in the liquid when all Cr is trivalent).

When log Cr^{2+}/Cr^{3+} is plotted vs. log f_{O_2} (Fig. 6) the data form a straight line that is fitted by the regression equation

$$\log\left[\frac{Cr^{2+}}{Cr^{3+}}\right] = -0.275 \times \log f_{O_2} - 2.598. \quad (2)$$

The reversal experiment (square in Fig. 6) was not used in the regression. The slope of this line (0.275) is in good agreement with the theoretically expected slope of 0.25 for a reaction involving the exchange of one electron (SH1976). We have calculated Cr^{2+}/Cr^{3+} for all of the Fe-free systems listed in Table 1 using Equation 1. In all cases, the slopes are consistent with the theoretically predicted value of 0.25 (Table 5) and are in good agreement with the results of Roeder and Reynolds (1991, Table 3) that were calculated based on chromite-melt equilibria. The good agreement between the measured and the theoretical slopes suggests that we can accurately calculate Cr^{2+}/Cr^{3+} in Fe-free systems using this procedure.

TABLE 5. Linear regression equations describing log$[Cr^{2+}/Cr^{3+}]$ vs. $-\log f_{O_2}$, calculated using Equation 1, for several Fe-free and Fe-bearing compositions

Composition	Temperature	Regression equation
FAD1	1320 °C	$\log[Cr^{2+}/Cr^{3+}] = 0.275 * [-\log f_{O_2}] - 2.59$
FAD3	1320 °C	$\log[Cr^{2+}/Cr^{3+}] = 0.274 * [-\log f_{O_2}] - 2.81$
FAS1	1320 °C	$\log[Cr^{2+}/Cr^{3+}] = 0.242 * [-\log f_{O_2}] - 2.05$
MORB1	1250 °C	$\log[Cr^{2+}/Cr^{3+}] = 0.286 * [-\log f_{O_2}] - 2.88$
MORB2	1200 °C	$\log[Cr^{2+}/Cr^{3+}] = 0.219 * [-\log f_{O_2}] - 2.34$
MORB3	1200 °C	$\log[Cr^{2+}/Cr^{3+}] = 0.241 * [-\log f_{O_2}] - 2.47$
BASALT*	1260 °C	$\log[Cr^{2+}/Cr^{3+}] = 0.276 * [-\log f_{O_2}] - 2.59$

* Unpublished data from J. Delano. Other compositions listed in Table 1.

Effect of Fe^{3+} on Cr^{2+}/Cr^{3+} in spinel-saturated basalts

The behavior of Cr in spinel-saturated glasses as a function of f_{O_2} is similar in Fe-free and Fe-bearing systems. Figure 7 shows that the Cr content of an Fe-bearing glass increases as f_{O_2} decreases, and the Cr content is independent of the total Cr in the system at any given f_{O_2}, just as it is in an Fe-free systems (Table 4). SH(1976), however, predicted that the presence of Fe^{3+} would have a significant effect on Cr^{2+}/Cr^{3+} in basaltic liquids and that Cr^{2+} would not exist in Fe-bearing magmas under terrestrial redox conditions (i.e., at QFM). Gaetani and Grove (1997) concluded, based on Cr-partitioning systematics into sulfide metal, that the dominant Cr species

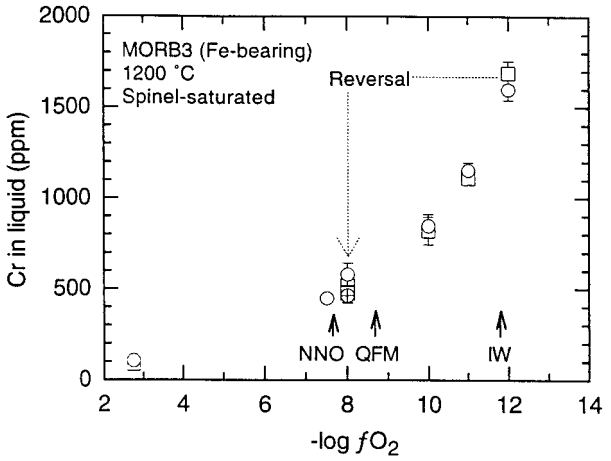

FIGURE 7. Plot of Cr content of spinel-saturated glasses from experiments performed on MORB3a (circles = 3000 ppm total Cr) and MORB3b (squares = 1500 ppm total Cr) as a function of f_{O_2}. Note that, like the Fe-free system, Cr content at spinel saturation is unaffected by total Cr. The symbols with crosses are the reversal experiments changed from IW to QFM after 24 h. The experiment at high f_{O_2} was not used because the spinel composition was very different from those at lower f_{O_2} (see text for discussion).

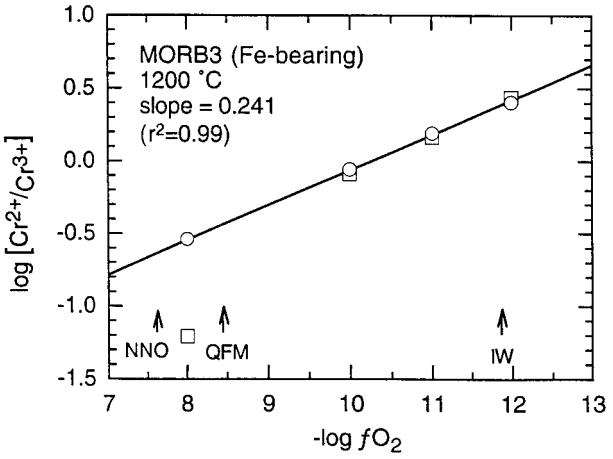

FIGURE 8. Plot of log $[Cr^{2+}/Cr^{3+}]$ vs. $-\log f_{O_2}$ for the MORB3 experiments shown in Fig. 7 (same symbols as in Figure 7) calculated using Equation 1. All Cr is assumed to be trivalent at NNO in Fe-bearing systems (see text). Note that Fe-free data also form a straight line with a slope very near to 0.25 in this plot. The reversal experiments and were not used in the regression calculation (see text).

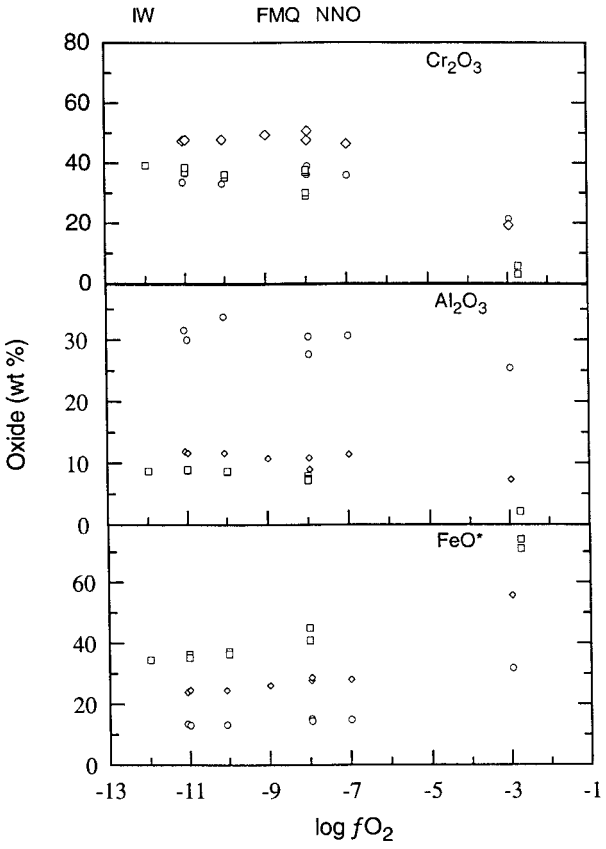

FIGURE 9. Plots of the compositions of spinels from experiments performed on MORB1 at 1175 °C (circles), MORB2 at 1200 °C (diamonds), and MORB3 at 1200 °C (squares). Note that the spinel compositions remain remarkably constant and only begin to change at oxygen fugacities above NNO.

is Cr^{3+} in their Fe-bearing system over an f_{O_2} range from IW to QFM. Because there is no reliable method at present to directly measure Cr^{2+}/Cr^{3+} in Fe-bearing systems, the extent of the effect of Fe on Cr systematics is poorly understood.

Using Equation 1, however, we can qualitatively evaluate the effect of Fe on Cr^{2+}/Cr^{3+} in spinel-saturated liquids. We have calculated log (Cr^{2+}/Cr^{3+}) from the data shown in Figure 7 using Equation 1 and have plotted the results against log f_{O_2} in Figure 8. We have chosen the Cr content of glass from the experiment performed at NNO as the Cr^{3+} content of the glass at spinel saturation (i.e., Cr_{min}). We have chosen NNO because the spinel compositions (and consequently the Cr^{3+} activity in the spinel) change little between IW and NNO but begin to change very rapidly at higher f_{O_2} (Fig. 9). Therefore, the activity of Cr^{3+} in the liquid (and consequently the Cr^{3+} content of the liquid) in equilibrium with the spinel should remain essentially constant in the f_{O_2} interval between IW and NNO, and NNO is the highest possible f_{O_2} before the rapid change in the spinel composition. We assume that the reversal experiments did not completely equilibrate and thus were omitted from the calculation of the slope. Because the Cr content in the liquid at QFM is very close to the Cr content at NNO, small analytical problems translate into large deviations in $\log(Cr^{2+}/Cr^{3+})$ calculated using Equation 1. Thus, the seemingly spurious data point at high f_{O_2} (QFM) was omitted from the regression as well. The slope of the line formed by the other data (0.241) is very close to the theoretically predicted value of 0.25.

We have calculated the Cr^{2+}/Cr^{3+} for several other Fe-bearing compositions, including those listed in Table 1, and the equations of these lines are listed in Table 5. Again, the slopes of these lines are close to the theoretically expected value of 0.25. If all of the Cr in the liquid at NNO were not trivalent, as we have assumed, the slope of the line in Figure 8 would be shallower owing to an over-estimation of the Cr^{3+} abundance.

The data shown in Figure 2 initially led us to the hypothesis that Cr^{2+} does not exist in the presence of Fe^{3+}, but this does not seem to be the case. The fact that the slopes in Figure 8 and Table 5 are approximately 0.25 qualitatively suggests that Fe does not exclude the presence of Cr^{2+} when the f_{O_2} is between IW and QFM. However, it appears that the presence of Fe^{3+} has suppressed the formation of Cr^{2+} so that its abundance starts to become significant ~3–4 log f_{O_2} units below where it is first observed in the Fe-free system. This discussion is predicated on the assumption that all Cr at NNO exists as Cr^{3+}, which is not true in the Fe-free system (Fig. 6). And Roeder and Reynolds (1991) estimated that only 70% of the Cr was trivalent in their Fe-bearing systems at QFM. However, our slopes of ~0.25 are in good agreement with the slopes determined by them, and if our assumption of no Cr^{2+} at NNO were seriously in error we

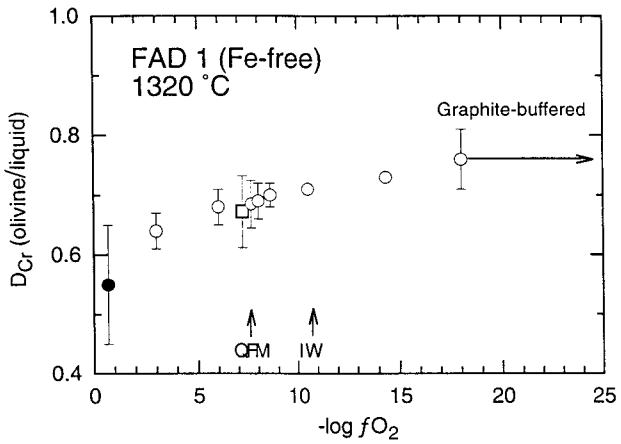

FIGURE 10. Plot of D_{Cr} as a function of f_{O_2} from the experiments performed on FAD1 that are shown in Figures 5 and 6. The point with an arrow represents the graphite-bearing experiment in which the f_{O_2} is unknown, but is thought to be less than 10^{-18} bar. The square is the reversal experiment. The presence of Cr metal in the graphite-bearing experiment implies that all Cr in the silicate is divalent.

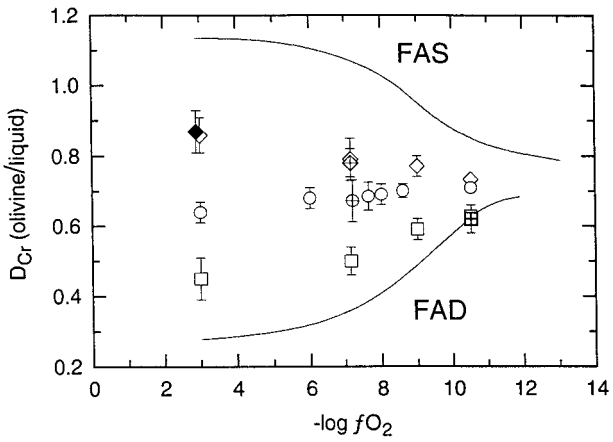

FIGURE 11. Plot of D_{Cr} as a function of f_{O_2} for the bulk compositions FAD1 (circles), FAD3 (squares), and FAS1 (diamonds). Note that Fe-loop and sealed tube experiments are not plotted. The lines are the approximate locations of the data trends interpolated to 1320 °C from the data in Figure 1. FAD3 and FAS1 were synthesized in an attempt to reproduce the experiments of Schreiber and Haskin at low temperatures.

would not calculate the theoretically predicted slope. The small difference between the conclusions of this study and those of Roeder and Reynolds (1991) is probably due to differences in bulk composition and/or temperature.

D_{Cr} olivine/liquid

The systematics in the previous section allow us to determine values for $D_{Cr^{2+}}$ and $D_{Cr^{3+}}$. The values of $D_{Cr^{2+}}$ were measured directly from the sealed silica-tube experiments and the Fe loop experiments, as discussed above. The redox conditions under which all Cr is trivalent is taken as the minimum Cr value of the curve in Figure 5, as discussed above. Figure 10 is a plot of D_{Cr} as a function of f_{O_2} for our Fe-free composition FAD1 (Table 1). For this liquid composition, D_{Cr} changes very little from experiments performed under redox conditions where Cr metal is stable ($\log f_{O_2} < -18$) to the highly oxidizing conditions of pure CO_2 ($\log f_{O_2} < -3$). D_{Cr} then abruptly drops from 0.64 to 0.55 in the f_{O_2} interval between $\log f_{O_2} = -3$ and air. This observation suggests that a significant amount of Cr^{6+} is present, which is assumed to be highly incompatible in olivine.

Figure 11 shows the measured values for D_{Cr} as a function of f_{O_2} at 1320 °C for all of the Fe-free compositions given in Table 1. Also shown on this diagram are the *D*-values measured by SH(1976) at 1350–1300 °C. Because SH(1976) did not perform experiments at 1320 °C, the *D*-values for the FAS system shown in Figure 11 are interpolated from the 1350 and 1300 °C data (Fig. 1). For the FAD system, the 1350 °C isotherm is depicted in Figure 11 because no experiments were run at 1320 °C but the effect of temperature is apparently small in this system (Fig. 1). Note that our results are consistent with those of SH(1976) at low f_{O_2}, but the two data sets deviate markedly at higher f_{O_2}.

Although the general shapes of the curves are similar (i.e., D_{Cr} increases with decreasing f_{O_2} in FAD and decreases in FAS), our data show a far more limited range in D_{Cr} at high f_{O_2} than would be expected, based on the systematics of SH(1976). An additional experiment on composition FAS1 (Table 1) was run at 1300 °C and the result is also plotted in Figure 11 (solid symbol). This experiment was performed in an attempt to directly reproduce the maximum value of D_{Cr} observed by SH(1976) ($D_{Cr} \approx 1.4$; Fig. 1). Our value of 0.87 for D_{Cr} at 1300 °C is indistinguishable from our value at 1320 °C and is considerably lower than that of SH(1976). Thus, the 1300 °C values for D_{Cr} in the system FAS from SH(1976) seem anomalously high.

The reason for the discrepancy between our results and those of SH(1976) is unclear. One possible explanation is the analytical difficulty posed by the presence of very small (<2 μm) spinel crystals, which can be difficult to detect in either reflected or transmitted light. Such spinels are very common as inclusions in the olivine grains of our experiments on this composition at high f_{O_2}, and could only be detected in backscattered electron (BSE) images at high magnification. Some of these spinels only appear as diffuse, bright regions in the cores of some olivine crystals in BSE images. Spinels of this size could not have been detected easily without the imaging systems available on newer generation microprobes, and could be the reason for the anomalously high D_{Cr} values measured by SH(1976) at low temperatures and high f_{O_2}.

Our *D*-values appear to disagree somewhat with the results of SH(1976) in the system FAD as well. SH(1976) did not perform an experiment at 1320 °C in the system FAD, so our results are not directly comparable to theirs. However, their values of D_{Cr} at high f_{O_2} do not change

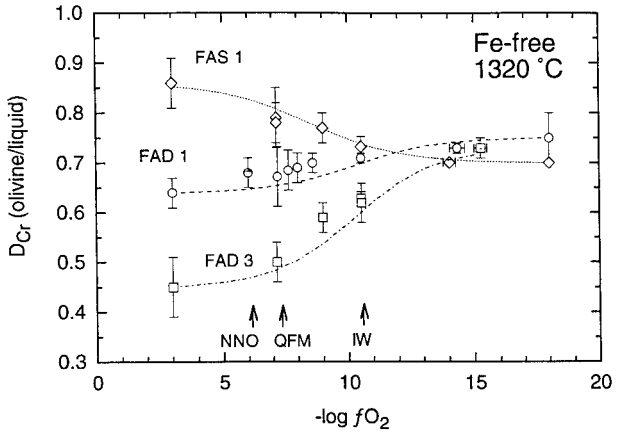

FIGURE 12. All data from Fe-free systems FAS1, FAD1, and FAD3 with calculated values for D_{Cr} (dashed lines) superimposed. The data was calculated using Equation 3, where $D_{Cr^{2+}}$ is taken as the measured value for D_{Cr} in the most reducing experiment and $D_{Cr^{3+}}$ is taken from the experiments run in pure CO_2. The good agreement between the calculated values and the measured values at intermediate f_{O_2} values demonstrates the internal consistency of the data.

significantly from 1450 to 1350 °C. Therefore, we would not have expected the value to begin to change so abruptly when the temperature is dropped by only 30 °C (to 1320 °C). We return to this issue when we discuss the effect of liquid composition on D_{Cr}.

Given our experimentally determined values for $D_{Cr^{2+}}$, $D_{Cr^{3+}}$, and an estimate of Cr^{2+}/Cr^{3+} of the liquids as a function of f_{O_2}, we can test our partitioning data for internal consistency. It is a simple matter to calculate a value for D_{Cr} by

$$D_{Cr} = X_{Cr^{2+}} \cdot D_{Cr^{2+}} + X_{Cr^{3+}} \cdot D_{Cr^{3+}} \quad (3)$$

where X is the mass fraction of Cr^{2+} or Cr^{3+} in the liquid. The results of these calculations for compositions FAD1, FAD3, and FAS1 are plotted in Figure 12. The close agreement between the measured D_{Cr} at intermediate f_{O_2} and those calculated as described above demonstrates the internal consistency of our intermediate-f_{O_2} data. This is a truly independent calculation because $X_{Cr^{2+}}$ and $X_{Cr^{3+}}$ are determined from the systematics of Cr solubility in spinel-saturated silicate melts.

The effect of liquid composition on D_{Cr} (olivine/liquid)

***D*$_{Cr^{3+}}$ (olivine/liquid).** Although significant differences exist in D_{Cr} among our experiments and those of SH(1976), both data sets indicate that D_{Cr} is sensitive to liquid composition, at least at high f_{O_2}. Our data allow us to quantify this variation more precisely because we have good estimates of individual values for $D_{Cr^{3+}}$ and $D_{Cr^{2+}}$ for each composition.

The partitioning behavior of trace elements depends, in part, on the availability of accommodating sites within the liquid structure. Several methods have been used to quantify the structure of silicate liquids based on their chemical composition (e.g., Si/O, NBO/T, optical basicity). We have arbitrarily chosen the commonly used ratio of the non-bridging O atoms to the tetrahedrally coordinated cations (NBO/T), according to the model of Mysen (1983), to quantify the change in liquid structure with changing composition. However, we have observed that the NBO/T parameter is highly correlated with the optical basicity model of Duffy (1993), so we expect either model to yield similar results.

Figure 13a is a plot of $D_{Cr^{3+}}$ as a function of NBO/T. The data from our Fe-free experiments at high f_{O_2} form a straight line described by the regression given in Figure 13a. The data plotted in Figure 13a are mostly from experiments performed at 1320 °C, with the exception of a single experiment performed at 1300 °C.

The data from SH(1976) have been superimposed on our results in Figure 13b, and in light of the foregoing discussion, the agreement is good. Within experimental uncertainty, four of the seven SH(1976) data points are in excellent agreement with our trend. The 1300 °C FAS experiment and the 1400 and 1450 °C FAD experiments fall off of the trend, however. We cannot reproduce the SH(1976) FAS result, so the discrepancy is not unexpected. The FAD experiments are more problematic. Although we are suspicious of the observed constancy of D_{Cr} over a 100 °C temperature interval in the FAD system, we do not know what the functional form of the trend depicted in Figure 13a should be. It appears to be linear in the NBO/T interval between 0.5 and 1.3, but there is no a priori reason to believe that it should remain linear. Perhaps the curve levels off at very high values of NBO/T (although see Fig. 13c). Regardless, it remains unclear whether SH(1976) experienced analytical or experimental problems in the system FAD or if $D_{Cr^{3+}}$ olivine/liquid becomes constant at high values of NBO/T. But with the notable exception of the 1300 °C FAS isotherm, we believe that a reasonable agreement exists between our two data sets.

Data from Fe-bearing systems show similar systematics. Figure 13c shows experimental data from Fe-bearing systems from this study (Table 5) and from the literature, which cover a considerable compositional and temperature range, and these data are compared to the trend defined by the Fe-free data from Figure 13b. We used simple criteria to select the data shown in Figure 13c. Useful Cr partitioning data must have uncertainties that are less than 10% relative and have values for the olivine-liquid Fe-Mg exchange (K_D; calculated assuming all Fe is ferrous) of 0.3 ± 0.02 (Roeder and Emslie 1970). Because values of K_D can vary significantly with liquid composition (Ford et al. 1983), we have only included those literature experiments having K_D values that agree well with prediction. K_D was estimated either by the Ford et al. (1983) parameterization for low-Ti liquids or the Jones (1988) parameterization for high-Ti lunar compositions. Of necessity, we chose experiments that were performed at f_{O_2} conditions at or above QFM so that most of the Cr

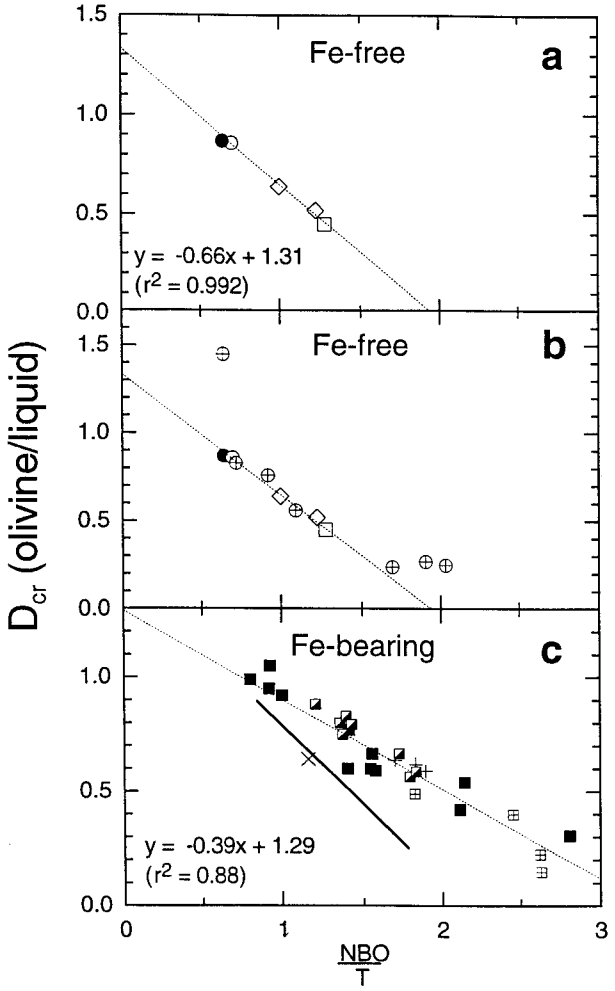

FIGURE 13. Plots of $D_{Cr^{3+}}$ vs. NBO/T (Mysen 1983). (**a**) Different symbols represent sets of experiments: open circles = FAS1 (1300 and 1320 °C); diamonds = FAD1 and FAD2; and squares = FAD3. The line is a linear regression through these data. (**b**) The data of SH(1976) (circles with crosses) superimposed on the data shown in a. Note that, in general, the SH(1976) data in b fall on or near the trend, except for the 1300 °C FAS point. (**c**) Results of Fe-bearing 1 atm experiments run between 1150 and 1450 °C (filled squares) from this study and the literature [half-filled squares represent data from Longhi and Pan (1989); *X* from Mikouchi et al. (1994); cross from Gaetani and Grove (1997)] as well as multianvil experiments from 5 to 15.5 GPa and 1726–2050 °C (squares with crosses). The line shows the trend of the Fe-free data, and the equation in the lower left corner is the linear regression equation through the Fe-bearing data.

was present as Cr^{3+} (see discussion of the effect of Fe^{3+} on Cr valence state below).

The high-f_{O_2} data from the Fe-bearing experiments form a good linear trend with NBO/T that is offset from the Fe-free experiments toward higher values of D_{Cr} (Fig. 13c). Although the data exhibit some scatter, the value for $D_{Cr^{3+}}$ olivine/liquid apparently can be predicted to within ±10% on the basis of the major-element composition of the basaltic liquid, in both Fe-free and Fe-bearing systems. The 1 bar experiments plotted in Figure 13c span a large temperature range (1150–1400 °C) indicating that knowledge of temperature is not required. Also included in Figure 13c are the results of multi-anvil experiments from Herzberg and Zhang (1996). These experiments were performed at pressures between 5 and 15.5 GPa and temperatures between 1726 and 2050 °C in Rhenium capsules. Nominally, the Re-ReO_2 buffer would be 2 log units above QFM (Pounceby and O'Neill 1996). Most of the ReO_2 will dissolve in the silicate liquid, and therefore the activity of ReO_2 may not be unity. Thus, 2 log units above QFM is probably an upper limit on f_{O_2}. Because there are no other species in the samples with a significant capacity to reduce the system, we assume that the f_{O_2} of the system was somewhere between NNO and QFM. The Herzberg and Zhang (1996) data fall on the trend of the 1 atm Fe-bearing experiments, suggesting that the relationship between NBO/T and $D_{Cr^{3+}}$ is also insensitive to pressure.

The variation in $D_{Cr^{3+}}$ exhibited with changing melt composition reflects the availability of network-modifying sites in the liquid (Schreiber 1976), which seems to be adequately quantified by NBO/T. Again, it is not clear why there is a simple linear relationship between NBO/T and $D_{Cr^{3+}}$, or if this linear relationship extends to extreme values of NBO/T. It is also not clear why there are two separate trends for Fe-free and Fe-bearing compositions. The existence of two trends might reflect the effect of Fe on the liquid structure and the availability of Cr^{3+}-accommodating sites in the liquid. Alternatively, the two trends might reflect crystal-chemical controls on Cr^{3+} partitioning into olivine. The data in Tables 2 and 3 indicate that insufficient Al occurs in the olivines to adequately charge balance the Cr^{3+}, either by substituting an Al^{3+} for Si^{4+} on tetrahedral sites or by substituting Al^{3+}, Cr^{3+}, and a vacancy for $3Mg^{2+}$ on octahedral sites. The vacancy substitution mechanism was demonstrated for Sc substitution into olivine by Nielsen et al. (1992) and Jones et al. (1995). In the Fe-free systems, Cr^{3+} presumably must pair with another Cr^{3+} to enter the olivine structure. In the Fe-bearing systems, however, Cr^{3+} might also pair with an Fe^{3+} cation. The overabundance of Fe^{3+} relative to Cr^{3+} could result in a higher value of $D_{Cr^{3+}}$ at a given value of NBO/T, in general agreement with the trends of Figure 13c.

***D*$_{Cr^{2+}}$ (olivine/liquid).** $D_{Cr^{2+}}$ has been determined for Fe-free systems by running experiments under very reducing conditions (i.e., sealed tube and Fe-loop experiments). Figure 14 shows that $D_{Cr^{2+}}$ correlates linearly both with $1/T$ (K) and with D_{Mg} (olivine/liquid), consistent with the results of Schreiber (1979) and Schreiber and Andrews (1980), but it does not correlate with NBO/T. It is not possible to run highly reducing experiments such as these in Fe-bearing systems without drastic changes in the composition of the melt resulting from Fe^0 precipitation. We must rely on the data of experiments run at oxygen fu-

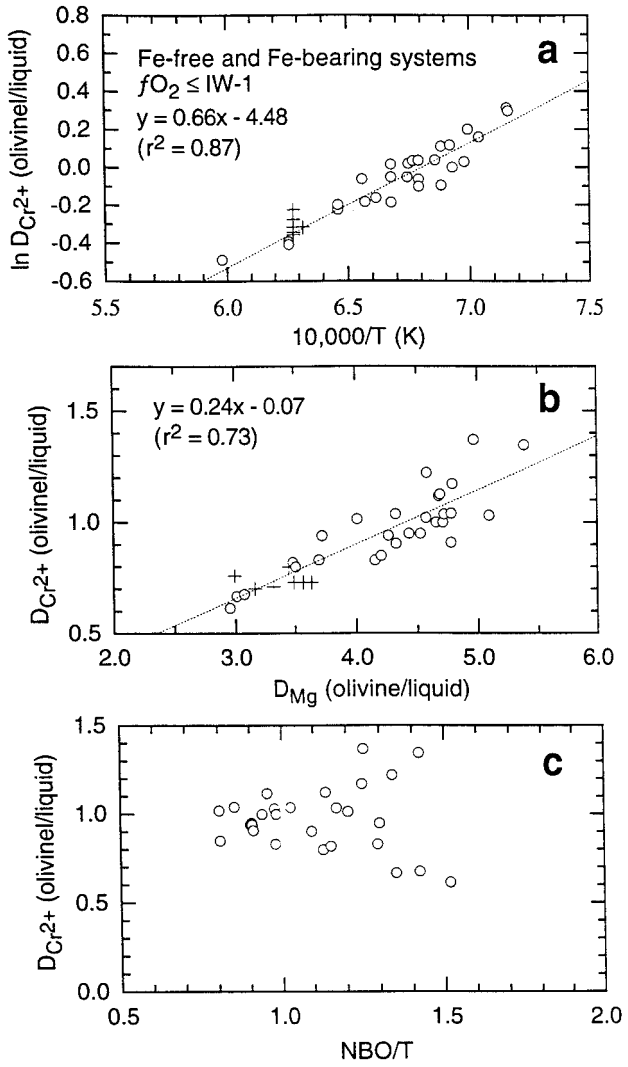

FIGURE 14. Plot of (**a**) ln $D_{Cr^{3+}}$ vs. 10 000/T(K) and (**b**) $D_{Cr^{2+}}$ vs. D_{MgO} for Fe-bearing (circles) and Fe-free (crosses) experiments from this study and from the literature. We assume that, under these redox conditions, all of the Cr is divalent. The regression equations for these data are shown on the diagrams. Note the good covariation of $D_{Cr^{2+}}$ with both of these parameters. (**c**) Plot of NBO/T vs. $D_{Cr^{2+}}$ for the same Fe-bearing data sets shown in a and b. Note that, in contrast to $D_{Cr^{3+}}$, $D_{Cr^{2+}}$ shows no systematic variation with NBO/T.

gacities ≤IW-1. From the equations listed in Table 3, 15–23% of the Cr in Fe-bearing systems will be trivalent at IW-1. Thus, the D_{Cr} should be dominated by $D_{Cr^{2+}}$. The results of experiments on Fe-bearing systems run at IW-1 from this study and from the literature are also plotted in Figure 14. These data are consistent with the Fe-free data run at lower f_{O_2}. It is not unexpected that ln $D_{Cr^{2+}}$ covaries linearly with 10 000/T (K) (Jones 1995) or, for that matter, D_{Mg} (olivine/liquid), which is also a function of temperature. The linear covariation between D_{Mg} and $D_{Cr^{2+}}$ was observed by Schreiber (1979) and has been observed for both divalent and trivalent cations (Jones 1995). However, $D_{Cr^{2+}}$ does not correlate with NBO/T as $D_{Cr^{3+}}$ does (Fig. 14c).

DISCUSSION

The partitioning behavior of Cr between basaltic liquids and olivine is complicated by the fact that natural systems may contain both Cr^{2+} and Cr^{3+}·$D_{Cr^{3+}}$ is sensitive to liquid composition whereas $D_{Cr^{2+}}$ is less sensitive to liquid composition but highly sensitive to temperature. The parameterization of these partition coefficients can easily explain the seemingly complex partitioning behavior of Cr between olivine and liquid. D_{Cr} can be easily predicted in most terrestrial basalts (i.e., those that crystallized near QFM) given only the liquid compositions. Conversely, D_{Cr} for lunar basalts or eucrites can be estimated using the regression equations shown in Figure 14.

But this new-found parameterization is of limited utility in modeling the igneous behavior of Cr. Figures 5 and 7 show that, in the presence of spinel, the Cr content of a basaltic liquid is ''buffered'' at a constant level. The addition or subtraction of Cr to a spinel-saturated basaltic liquid has no effect on the Cr content of the liquid as long as spinel is present. Thus, in the presence of spinel, the Cr content of a crystallizing basaltic liquid cannot be predicted using mathematical models that treat Cr as a ''common'' trace element that is either excluded or incorporated into silicate minerals according to a bulk distribution coefficient (e.g., Rayleigh fractionation). Instead, the Cr-saturation concentrations reflect spinel compositions that, in turn, reflect the changing composition of a basaltic liquid during fractionation (e.g., Roeder and Reynolds 1991).

Our results also bear on Cr^{2+} partitioning into spinel grown from basaltic liquids. It is thought that Cr^{2+} cannot partition significantly into spinel because it cannot compete for sites with other divalent cations (Mao and Bell 1975). We propose that Cr^{2+} may be as compatible in Cr-rich spinel as Mg or Fe [i.e., $D_{Cr^{2+}}$ (spinel/liquid) = 1–2], but the Cr^{2+} content of spinel is simply too low to measure accurately. For example, we calculate 1800 ppm Cr^{2+} in the FAD1 liquid at IW (Fig. 5). Cr^{2+} would contribute 0.18–0.32 wt% Cr to a spinel containing >22 wt% Cr, assuming a $D_{Cr^{2+}}$ (spinel/liquid) of 1–2. Given present analytical constraints, it would be difficult to resolve this small amount of Cr^{2+} in spinel based on stoichiometry. The problem becomes worse in Fe-bearing spinels in light of the assumptions regarding spinel stoichiometry and Fe^{2+}/Fe^{3+} that must also be made. In addition, the demonstration by Li et al. (1995), that spinels can be produced which contain a substantial amount (~80%) of the end-member component Cr_3O_4, requires that Cr^{2+} not be automatically excluded from the spinel structure. Although Cr^{2+} may be compatible in the spinel structure, we emphasize that Cr^{3+} controls the stability of chromian spinels in natural basaltic systems.

Conclusions

Our suspicions regarding the validity of the partition coefficients measured by SH(1976) are confirmed, but only for their 1300 °C data at high f_{O_2} in the system FAS. Otherwise, there is close agreement between the two data sets at low f_{O_2}, suggesting that the SH(1976) experiments gave a close approach to equilibrium. The fact that most of the SH(1976) partition coefficients at high f_{O_2} ($\sim 10^{-3}$) fall along the $D_{Cr^{3+}}$ vs. NBO/T trend defined by our experiments increases our confidence in the bulk of their high f_{O_2} data as well, although some uncertainty remains regarding the distribution behavior of Cr^{3+} in liquids having high values of NBO/T. The consistency of the two data sets and the internal consistency of the Cr^{2+}/Cr^{3+} measurements and the distribution data add further confidence to both data sets.

The partitioning behavior of Cr between olivine and liquid in the Fe-bearing systems shown in Figure 2 can also be explained by our results. D_{Cr} is not affected by f_{O_2} because $D_{Cr^{3+}}$ and $D_{Cr^{2+}}$ coincidentally happen to be the same for these compositions. $D_{Cr^{3+}}$ from Gaetani and Grove (1997; Table 8) is 0.642 and $D_{Cr^{2+}}$ at 1350 °C, calculated using Equation 6, is 0.66. $D_{Cr^{3+}}$ from Makouchi et al. (1994) is 0.62 at 1400 °C, and $D_{Cr^{2+}}$ at this temperature, again calculated using Equation 6, is 0.59. Both of these measured values of $D_{Cr^{3+}}$ are also consistent with our correlation between $D_{Cr^{3+}}$ and NBO/T.

Although we can make qualitative statements regarding the effect of Fe^{3+} on Cr in Fe-bearing systems, there still remains a need to accurately quantify the magnitude of this effect before we can fully understand Cr behavior in natural basalts. Finally, because the Cr content of a basaltic liquid is ''buffered'' in the presence of spinel, Rayleigh fractionation models cannot be applied to Cr. To model the behavior of Cr in spinel-saturated liquids, the dependence of the Cr-saturation abundance on f_{O_2}, temperature, spinel, and liquid composition must be understood. For now, we must rely on experimentally derived Cr-saturation abundances to model Cr in basaltic systems.

Acknowledgments

Thanks to J. Delano for spurring interest in Cr partitioning and also for the use of his laboratory equipment and materials. We also thank John Longhi for loaning us experimental samples for Cr analyses. Thanks to Gordon McKay for providing unpublished data. We appreciate the detailed reviews of P.L. Roeder, H.D. Schreiber, G.A. Gaetani, and R.W. Luth, which greatly improved the manuscript. The meticulous editorship of R.F. Dymek also improved the quality of the manuscript. Discussions with J. Delaney, G.C. Ulmer, D.J. Lindstrom, and H.D. Schreiber also have been of great help during this work. This research was funded by NASA grants NAGW 3357 (J.W. Delano) and 344-31-20-18 (J.H. Jones).

References cited

Akella, J. Williams, R.J., and Mullins, O. (1976) Solubility of Cr, Ti, and Al in co-existing olivine, spinel, and liquid at 1 atm. Proceedings of the Lunar Science Conference, 7, 1179–1194.

Barnes, S.J. (1986) The distribution of chromium among orthopyroxene, spinel, and silicate liquid at atmospheric pressure. Geochimica et Cosmochimica Acta, 50, 1889–1909.

Bell, P.M. (1970) Analyses of olivine crystals in Apollo 12 rocks. Carnegie Institution of Washington Yearbook, 69, 228–229.

Duffy, J.A. (1993) A review of optical basicity and its applications to oxide systems. Geochimica et Cosmochimica Acta, 57, 3961–3970.

Delano, J.W. (1986) Pristine lunar glasses: Criteria, data, and implications. Proceedings of the Sixteenth Lunar and Planetary Science Conference, Journal of Geophysical Research, 91, B4, D201–D213.

Ford, C.E., Russell, D.G., Craven, J.A., and Fisk, M.R. (1983) Olivine-liquid equilibria: Temperature, pressure, and composition dependence of the crystal/liquid cation partition coefficients for Mg, Fe^{2+}, Ca, and Mn. Journal of Petrology, 24, 256–265.

Gaetani, G.A. and Grove, T.L. (1997) Partitioning of moderately siderophile elements among olivine, silicate melt, and sulfide melts: Constraints on core formation in the Earth and Mars. Geochimica et Cosmochimica Acta, 61, 1829–1846.

Grove, T.L. (1981) Use of FePt alloys to eliminate the iron loss problem in 1-atmosphere gas mixing experiments: theoretical and practical considerations. Contributions to Mineralogy and Petrology, 78, 298–304.

Herzberg, C. and Zhang, J. (1996) Melting experiments on anhydrous peridotite KLB-1: Compositions of magmas in the upper mantle and transition zone. Journal of Geophysical Research, 101, 8271–8296.

Hillgren, V.J. (1993) Partitioning behavior of moderately siderophile elements in Ni-rich systems: Implications for the Earth and Moon. Ph.D. dissertation, University of Arizona, Tucson, AZ.

Huebner, J.S., Lipin, B.R., and Wiggins, L.B. (1976) Partitioning of chromium between silicate crystals and melts. Proceedings of the Lunar Science Conference, 7, 1195–1220.

Jones, J.H. (1988) Partitioning of Mg and Fe between olivine and liquids of lunar compositions: The roles of composition, pressure, and Ti speciation. Lunar and Planetary Science Conference, 19, 561–562.

——— (1995) Trace element partitioning. Rock physics and phase relations, A handbook of physical constants, AGU Reference Shelf, 3, 73–104.

Jones, J.H. and Delano, J.W. (1989) A three-component model for the bulk composition of the Moon. Geochimica et Cosmochimica Acta, 53, 513–527.

Jones, J.H., Lindstrom, D.J., Lauer, H.V., Paslick, C.R., and Christoffersen, R. (1995) Scandalous Sc partitioning: Unnatural adherence to Henry's law and the possibility of tetrahedral Sc. Eos, 76, 705.

Jurewicz, A.J.G., Mittlefehldt, D.W., and Jones, J.H. (1993a) Experimental partial melting of the Allende (CV) and Murchison (CM) chondrites and the origin of asteroidal basalts. Geochimica et Cosmochimica Acta, 57, 2123–2139.

Jurewicz, A.J.G., Williams, R.J., Le, L., Lofgren, G., Lanier, A., Carter, W., and Roshko, A. (1993b) Technical Update: JSC system using a solid electrolytic cell in a remote location to measure oxygen fugacities in CO/CO_2 controlled-atmosphere furnaces. NASA Technical Memorandum 104774.

Jurewicz, S.R., Jones, J.H., and Fegley, B. Jr. (1995) Experimental partitioning of Zr, Nb, and Ti between platinum group metals and silicate liquid: Implications for the origin of refractory metal nuggets in carbonaceous chondrites. Earth and Planetary Science Letters, 132, 183–198.

Li, J., O'Neill, H., and Seifert, F. (1995) Subsolidus phase relations in the system $MgO\text{-}SiO_2\text{-}Cr\text{-}O$ in equilibrium with metallic Cr, and their significance for the petrochemistry of Chromium. Journal of Petrology, 36, 107–132.

Longhi, J. and Pan, V. (1989) The parent magmas of SNC meteorites. Proceedings of the Lunar and Planetary Science Conference, 19, 451–464.

Mao, H.K. and Bell, P.M. (1975) Crystal field effects in spinel: oxidation states of iron and chromium. Geochimica et Cosmochimica Acta, 39, 865–874.

Mikouchi, T., McKay, G., and Le, L. (1994) Cr, Mn, and Ca distributions for olivine in angritic systems: Constraints on the origins of Cr-rich and Ca-poor core olivine in angrite LEW87051. Lunar and Planetary Science, 25, 907–908.

Murck, B.W. and Campbell, I.H. (1986) The effects of temperature, oxygen fugacity and melt composition on the behavior of chromium in basic and ultrabasic rocks. Geochimica et Cosmochimica Acta, 50, 1871–1887.

Mysen, B.O. (1983) The structure of silicate melts. Annual Reviews of Earth and Planetary Sciences, 11, 75–97.

Nielsen, R.L., Gallahan, W.E., and Newberger, F. (1992) Experimentally determined mineral-melt partition coefficients for Sc, Y, and REE for olivine, orthopyroxene, pigeonite, magnetite, and ilmenite. Contributions to Mineralogy and Petrology, 110, 488–499.

Pouchou, J. and Pichoir, F. (1991) Quantitative analyses of homogeneous or stratified microvolumes applying the model ''PAP''. In K.F.J. Heinrich and D.E. Newbury, Eds., Electron probe quantitation. Plenum Press, New York.

Pownceby, R. and O'Neill, H. (1994) Thermodynamic data for redox reactions at high temperatures and pressures; IV, calibration of the Re-ReO_2 oxygen buffer from EMF and NiO plus Ni-Pd redox sensor measurements. Contributions to Mineralogy and Petrology, 118, 130–136.

Robie, R.A., Hemingway, B.S., and Fisher, J.R. (1978) Thermodynamic properties of minerals and related substances at 298.15K and 1 bar (10^5 pascals) pressure and at higher temperatures. U.S. Geological Survey Bulletin, 1452.

Roeder, P.L. and Emslie, R.F. (1970) Olivine-liquid equilibria. Contributions to Mineralogy and Petrology, 29, 275–289.

Roeder, P.L. and Reynolds, I. (1991) Crystallization of chromite and chromite solubility in basaltic melts. Journal of Petrology, 32, 909–934.

Schreiber, H.D. (1976) The experimental determination of redox states, properties, and distribution of chromium in silicate phases and application to basalt petrogenesis, 221 p. Ph.D. dissertation, University of Wisconsin, Madison. (available from University Microfilms, Ann Arbor, Michigan).

Schreiber, H.D. (1979) Experimental studies of nickel and chromium partitioning into olivine from synthetic basaltic melts. Proceedings of the Lunar Science Conference 10, 509–516.

Schreiber, H.D. and Andrews, S.M (1980) Chromium in synthetic basalts: understanding the roles of Cr(III) and Cr(II). Lunar and Planetary Science, 11, 997–999.

Schreiber, H.D. and Haskin, L.A. (1976) Chromium in basalts: Experimental determination of redox states and partitioning among silicate phases. Proceedings of the Lunar Science Conference, 7, 513–538.

Taylor, S.R. (1975) Lunar Science: A Post Apollo View. Pergamon Press, Elmsford, New York, 372 p.

Walker, D., Longhi, J., Lasaga, A.C., Stolper, E.M., Grove, T.L., and Hays, J.F. (1977) Slowly cooled microgabbros 15555 and 15065. Proceedings of the Lunar Science Conference, 8, 1521–1547.

Manuscript received May 13, 1997
Manuscript accepted March 9, 1998
Paper handled by Robert W. Luth